

# Collective oscillations in optical matter

F. J. García de Abajo<sup>1</sup>

<sup>1</sup>*Instituto de Óptica - CSIC, Serrano 121, 28006 Madrid, Spain*

*E-mail: jga@io.cfmac.csic.es*

## Abstract

Atom and nanoparticle arrays trapped in optical lattices are shown to be capable of sustaining collective oscillations of frequency proportional to the strength of the external light field. The spectrum of these oscillations determines the mechanical stability of the arrays. This phenomenon is studied for dimers, strings, and two-dimensional planar arrays. Laterally confined particles free to move along an optical channel are also considered as an example of collective motion in partially-confined systems. The fundamental concepts of dynamical response in optical matter introduced here constitute the basis for potential applications to quantum information technology and signal processing. Experimental realizations of these systems are proposed.

## INTRODUCTION

Periodic standing light patterns created by coherent laser beams offer the possibility to trap objects ranging from single atoms [1] to micron-size particles [2, 3], forming ordered arrays that can be viewed as artificial crystals with the periodicity of the optical field. Starting from the equilibrium configuration of an ordered array with one particle per lattice site, the perturbation produced by slightly displacing one of the particles will be transmitted to the others via their mutual electromagnetic interaction, which is a complex function of the particles positions. This results in collective motion of the particles that resembles phonon vibrations in crystals and that we regard as collective oscillations in optical matter.

In this context, the interaction of ultracold atoms with optical lattices has recently attracted considerable attention because of its potential use for quantum information technology, in which the realization of trapping of no more than one atom per lattice site has been an important benchmark [1]. Using light tuned close to some atomic resonance, strong light-induced interaction between atoms trapped in different sites can take place even for commonly employed lattice periods of the order of  $1\text{ }\mu\text{m}$ , as suggested by recent observations in optical cavities under atom-cavity resonance conditions [4, 5]. These interatomic interactions are the driving force of the collective oscillations considered here, which for reasonably-cold atoms offer a potentially practical realization of quantum gates [6] involving large numbers of qubits.

Early attempts to bind small particles using light forces [2, 3, 7, 8, 9, 10] led to the development of optical tweezers [7, 10], capable of trapping and aligning objects ranging from micro-organisms [10] to metallic nanoparticles [11, 12]. Furthermore, holographic tweezers have been developed to trap tailored arrays of micron-size objects [13, 14] that offer an excellent playground to test many of the concepts discussed below. Manipulation of micro-particles using plasmons has been recently demonstrated as well [15], whereas fine tuning of nanoparticle positions has been theoretically proved to be realizable by coupling to plasmonic nanostructures [16].

Mutual inter-particle interaction induced by external illumination has been shown to lead to interesting effects such as configurational bistability in pairs of spheres [17] and crystallization in linear particle arrays trapped at the focus of counter-propagating lasers [18]. A close relative of the oscillations studied here are those of colloidal crystals [19],

mediated by electrostatic interaction similar to phonons in ionic crystals.

Here, we examine the collective oscillation modes of atoms and particles trapped in optical lattices. For atomic lattices, strong inter-atomic interaction effects are predicted in the oscillation spectrum near atomic absorption resonances. The particle dimer is studied first as a tutorial example. For extended systems, long-range  $1/r$  dynamical interaction between polarized atoms or particles is shown to give rise to soft modes observed in particular in one-dimensional (1D) periodic arrangements. Finally, periodic arrays confined within a 1D well are shown to exhibit imaginary collective-motion eigenfrequencies for some ranges of the particles spacing, thus revealing instabilities that preclude structural transformations.

## THEORETICAL BACKGROUND

We start by analyzing collective motion of small particles such as atoms, molecules or nanoparticles that respond to electromagnetic fields basically as induced dipoles driven by their polarizability  $\alpha(\omega)$ , where  $\omega$  is the light frequency. The time-averaged force acting on one of such particles in the presence of an external electric field  $\mathbf{E}^{\text{ext}}(\mathbf{r}, t) = 2 \Re\{\mathbf{E}^{\text{ext}}(\mathbf{r}) \exp(-i\omega t)\}$  is readily obtained from the integral of Maxwell's stress tensor on a small sphere surrounding the particle. One finds [20]

$$\mathbf{F} = 2 \Re \left\{ \alpha \sum_l E_l^{\text{ext}} [\nabla E_l^{\text{ext}}]^* \right\} = -\nabla V - 2 \Im\{\alpha\} \Im \left\{ \sum_l E_l^{\text{ext}} [\nabla E_l^{\text{ext}}]^* \right\}, \quad (1)$$

where  $l$  labels Cartesian coordinates,  $V(\mathbf{r}) = -\Re\{\alpha\}|\mathbf{E}^{\text{ext}}(\mathbf{r})|^2$  acts as an effective potential (i.e., the particle can be trapped in regions of low or high electric field strength when  $\Re\{\alpha\}$  is negative or positive, respectively), the second term in the right hand side of Eq. (1) describes the so-called radiation pressure, and we use Gaussian units throughout this paper.

Focusing on atoms, the frequency-dependent atomic polarizability near a resonance at frequency  $\omega_0$  with no decay channels other than radiative takes a simple form compatible with the optical theorem condition  $\Im\{-1/\alpha\} = 2k^3/3$  [21]:

$$\alpha(\omega) = \frac{3c^3\Gamma/2\omega_0^2}{\omega_0^2 - \omega^2 - i\Gamma\omega^3/\omega_0^2} \approx \frac{3c^3\Gamma/4\omega_0^3}{\omega_0 - \omega - i\Gamma/2}, \quad (2)$$

where  $k = \omega/c$  is the momentum of light in free space,  $\Gamma$  is the resonance frequency width, and the last approximation is valid for  $\Gamma \ll \omega_0$  and  $\omega$  near the resonance. Furthermore, our analysis assumes low-enough light intensities to exclude saturation effects near resonance, which would require to go beyond linear response approximation.

When several particles placed in vacuum are considered, their induced dipoles  $\mathbf{p}_j$  express the response to the external field plus the field scattered by the other particles, that is,

$$\mathbf{p}_j = \alpha \left[ \mathbf{E}^{\text{ext}}(\mathbf{r}_j) + \sum_{j' \neq j} G(\mathbf{r}_j - \mathbf{r}_{j'}) \mathbf{p}_{j'} \right], \quad (3)$$

where  $\mathbf{r}_j$  labels particle positions and an  $\exp(-i\omega t)$  time dependence is understood. The  $3 \times 3$  matrix

$$G(\mathbf{r}) = \left( k^2 + \nabla \otimes \nabla \right) \frac{e^{ikr}}{r} = A - \frac{B}{r^2} \mathbf{r} \otimes \mathbf{r}, \quad (4)$$

with coefficients

$$A = \frac{e^{ikr}}{r^3} \left[ (kr)^2 + ikr - 1 \right], \quad (5)$$

$$B = \frac{e^{ikr}}{r^3} \left[ (kr)^2 + 3ikr - 3 \right], \quad (6)$$

describes the electric field produced at the position  $\mathbf{r}$  by a dipole at the origin. All particles are considered to be equal for simplicity. The force acting on the particle at  $\mathbf{r}_j$  is then obtained from Eq. (1) by adding the scattered electric field  $\sum_{j' \neq j} G(\mathbf{r} - \mathbf{r}_{j'}) \mathbf{p}_{j'}$  to  $\mathbf{E}^{\text{ext}}(\mathbf{r})$ . Up to here, our analysis follows previous developments of optical forces acting on small particles described through their dipolar response [22, 23]. This type of formalism can only be applied to particles that are small with respect to both the wavelength and their separation. However, its extension to include multipolar terms in the interaction between neighboring particles has been successfully carried out both for axially-symmetric particles using 3D multipolar expansions [24] and for objects with translational invariance using 2D multipoles [25, 26].

It is easy to see that the dynamics can no longer be obtained from an effective potential  $V$ , even in the absence of radiation pressure. This is a manifestation of the fact that we are dealing with open systems in which the photon bath provided by the external field can add (remove) energy to (from) the motion of the particles.

## OPTICAL DIMER

We shall discuss first a simple atomic dimer system that illustrates the effect of strong inter-atomic interaction near an absorption resonance. Optical binding in a dimer has been

extensively studied both theoretically [27] and experimentally [2, 17], but here we shall focus on the dynamical aspects of such system.

An optical lattice will be considered to be formed by three pairs of equal-intensity counter-propagating lasers that define an orthogonal  $xyz$  frame, with their linear polarizations as shown in the lower inset of Fig. 1. The external electric field produced by the lasers is then given by

$$\mathbf{E}^{\text{ext}}(\mathbf{r}, t) = 4 \Re \left\{ E_0 e^{-i\omega t} \right\} [\sin(kz) \hat{\mathbf{x}} + \sin(kx) \hat{\mathbf{y}} + \sin(ky) \hat{\mathbf{z}}],$$

where  $E_0$  is the electric field amplitude of each laser. For  $\omega > \omega_0$  [see Eq. (2)], the atomic polarizability is essentially negative, as shown in the upper inset of Fig. 1, which represents the polarizability of Eq. (2) scaled to the wavelength ( $\alpha/\lambda^3$ ), so that the two atoms under consideration can be trapped at contiguous minima of the electric field (light regions in the lower inset).

The oscillation frequencies, as derived from Newton's equation for infinitesimal displacements from equilibrium positions, reduce after lengthy, straightforward algebra from Eqs. (1) and (3) to

$$\Omega_1^\pm = \frac{|E_0|k}{\sqrt{M}} \sqrt{8 \Re \left\{ \frac{-1}{\alpha^{-1} \pm A} \right\}} \quad (7)$$

and

$$\Omega_2^\pm = \frac{|E_0|k}{\sqrt{M}} \sqrt{8 \Re \left\{ \frac{-1}{\alpha^{-1} \pm (A - B)} \right\}}, \quad (8)$$

where  $M$  is the atomic mass,  $A = -8(\pi^2 + i\pi - 1)/\lambda^3$ , and  $A - B = 16(i\pi - 1)/\lambda^3$ , according to the definitions of Eqs. (5) and (6) for a dimer spacing  $r = \lambda/2$ . The light-frequency dependence of these oscillations is shown in Fig. 1, along with schematic representations of directions of motion for the modes, which illustrate how different orthogonal directions are decoupled. Modes of frequency  $\Omega_1^\pm$  and  $\Omega_2^\pm$  are doubly and singly degenerate, respectively, and they are represented by solid and dashed curves.

The dimer oscillation frequencies deviate considerably from the single atom case (dotted curve) as a result of inter-atomic interaction driven by the  $\omega_0$  resonance. Interestingly, this interaction pushes the range of instability of the dimer (signaled by some imaginary eigenfrequency  $\Omega$ ) slightly towards the  $\omega > \omega_0$  region as compared to the single atom.

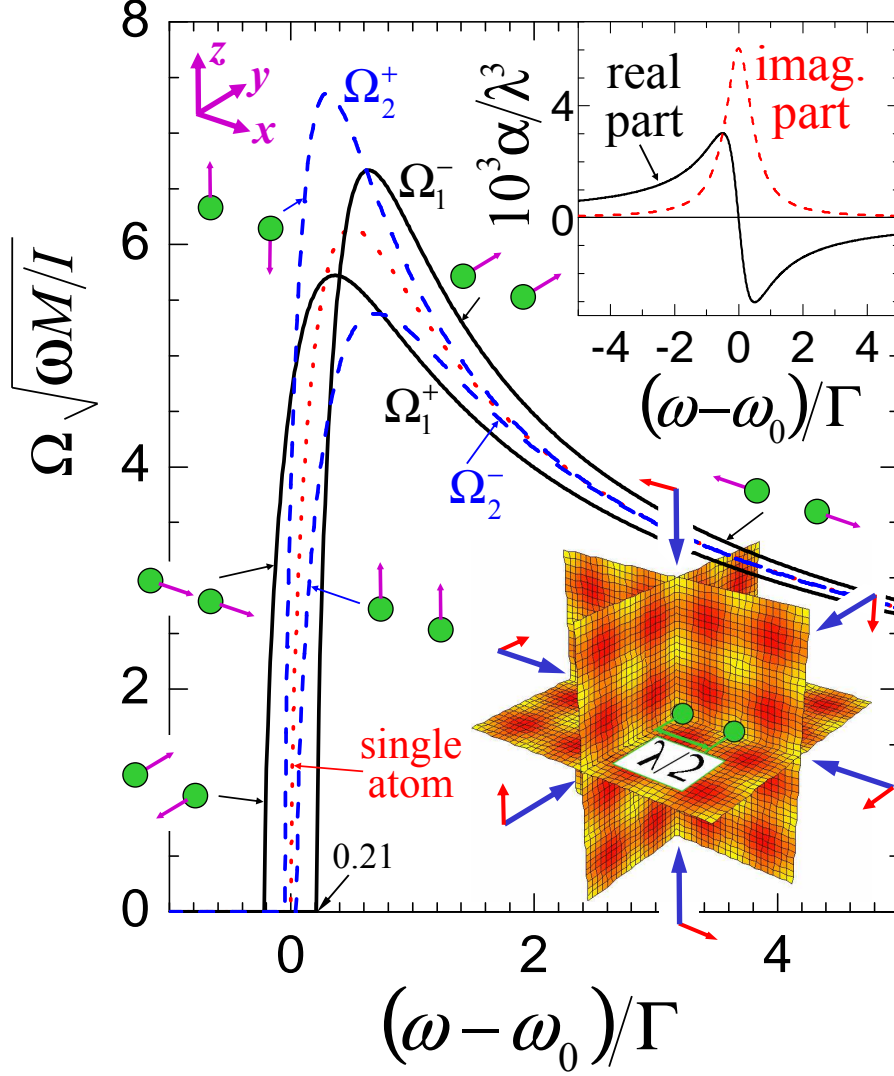


FIG. 1: Oscillation frequencies of two identical atoms trapped in contiguous wells of an optical lattice as a function of light frequency  $\omega$  near an atomic resonance  $\omega_0$ . The lattice is set up by three pairs of counter-propagating lasers of direction and (linear) polarization as shown in the lower inset. The wells are a distance  $\lambda/2$  apart, where  $\lambda = 2\pi c/\omega$  is the light wavelength. The atomic polarizability  $\alpha$  (upper inset) is obtained by assuming that radiative decay is the dominant contribution to the resonance width  $\Gamma$  [see Eq. (2)]. The oscillation frequency  $\Omega$  is normalized using the atom mass  $M$  and the intensity of each beam  $I$ . The oscillations take place around equilibrium positions corresponding to the vanishing of the electric field strength (yellow regions in lower inset). Six oscillation modes are obtained: two pairs of doubly-degenerate modes (solid curves) and two nondegenerate modes (dashed curves). The relative directions of motion of the atoms in the dimer are indicated by arrows for each of the modes. The oscillation frequency of a single trapped atom is given for reference (dotted curve).

Optical forces scale linearly with light intensity, and therefore, the oscillation frequencies are proportional to the strength of the applied electric field. This allows us to represent those frequencies normalized to the light intensity flux per laser,  $I = |E_0|^2 c / 2\pi$ . For instance, single Rb atoms ( $M = 85.46$  amu) near their 780 nm resonance ( $\Gamma = 2\pi \times 4$  MHz [28, 29]) will oscillate with frequency  $\Omega \approx 0.36$  MHz for  $I = 10$  mW/cm<sup>2</sup> lasers tuned to  $\omega = \omega_0 + 2\Gamma$ , which corresponds to a temperature of  $\approx 17$   $\mu$ K. Notice that  $\Omega \ll \Gamma$ , so that Doppler shifts can be safely neglected at this relatively high laser intensity, for which the atomic motion can be described classically, although saturation effects could be an issue [9].

## PERIODIC ARRAYS

Oscillations in periodic configurations of extended arrays can be studied by introducing small perturbations in Eq. (3) for specific momentum  $\mathbf{q}$ , corresponding to a displacement of every particle  $j$  around its equilibrium position  $\mathbf{r}_j$  given by  $\mathbf{u}_j = \mathbf{u}_{\mathbf{q}} \exp(i\mathbf{q} \cdot \mathbf{r}_j)$ . For small perturbations, the electromagnetic forces scale linearly with the displacement  $\mathbf{u}_{\mathbf{q}}$ , so that one obtains an equation of motion of the form

$$\Re\{\Sigma_{\mathbf{q}}\} \mathbf{u}_{\mathbf{q}} = -M\Omega_{\mathbf{q}}^2 \mathbf{u}_{\mathbf{q}}, \quad (9)$$

where  $M$  is the particle mass. Three branches of the oscillation frequency  $\Omega_{\mathbf{q}}$  are obtained in general out of the eigenvalues of the force constants matrix  $\Sigma_{\mathbf{q}}$ .

### 1D arrays

We shall first focus on blue-detuned systems, in which the particle polarizability has negative real part, so that the unperturbed particles sit at light intensity minima. Then, the force constants matrix reduces to

$$\Sigma_{\mathbf{q}} = |E_0|^2 k^2 \mathbf{C}^+ \frac{1}{\frac{1}{\alpha} - G_{\mathbf{q}}} \mathbf{C},$$

where

$$G_{\mathbf{q}} = \sum_{j \neq 0} e^{-i\mathbf{q} \cdot \mathbf{r}_j} G(\mathbf{r}_j) \quad (10)$$

is the sum of the dipole-dipole interaction extended over lattice sites  $\mathbf{r}_j$ , and  $\mathbf{C}$  is a dimensionless matrix that depends on the specific orientations and polarizations of the lasers setting up the optical lattice.

In particular, we shall consider a 1D infinite string formed by the same kind of blue-detuned atoms as in Fig. 1, with one atom trapped at each minimum of the electric-field along the  $\langle 111 \rangle$  direction of the same optical lattice. The oscillation frequencies are then labeled by the longitudinal momentum  $q$ . Displacements parallel ( $\parallel$ ) and perpendicular ( $\perp$ ) to the array turn out to be decoupled. We find the following analytical expression for the oscillation frequencies, similar in structure to Eqs. (7) and (8):

$$\Omega_q^\sigma = \frac{|E_0|k}{\sqrt{M}} \sqrt{8 \Re \left\{ \frac{-1}{\alpha^{-1} - G_q^\sigma} \right\}},$$

where  $\sigma = \parallel, \perp$  in each case, the lattice sums reduce to

$$G_q^\parallel = 4 \sum_{j=1}^{\infty} \cos(qaj) \frac{e^{ikaj}}{(aj)^3} (1 - ikaj) \quad (11)$$

and

$$G_q^\perp = 2 \sum_{j=1}^{\infty} \cos(qaj) \frac{e^{ikaj}}{(aj)^3} [(kaj)^2 + ikaj - 1], \quad (12)$$

and  $a = \sqrt{3}\lambda/2$  is the period of the array, so that  $ka = \sqrt{3}\pi$ .

Fig. 2 shows results obtained using this formalism within the first Brillouin zone in  $q$  space. Soft modes of zero frequency can be observed in the degenerate oscillations along directions transversal to the string, giving rise to large group velocities. This results from phase accumulation in the long-range inter-atomic interaction within Eq. (12), which diverges as  $\ln |\varphi \pm qa|$  near  $\mp qa = \varphi = (2 - \sqrt{3})\pi$ . This logarithmic divergence is obviously destroyed when the string is finite, regardless its length, and therefore, it cannot lead to permanent distortions of the lattice from the equidistant array configuration.

### Beyond the dipole approximation in 2D arrays

For particles of non-negligible size compared to the wavelength, multipoles beyond dipoles may become important. This situation can be described by a relation similar to Eq. (3), where  $\mathbf{p}$  is then understood as a vector of multipolar amplitudes and  $\alpha$  is the multipolar

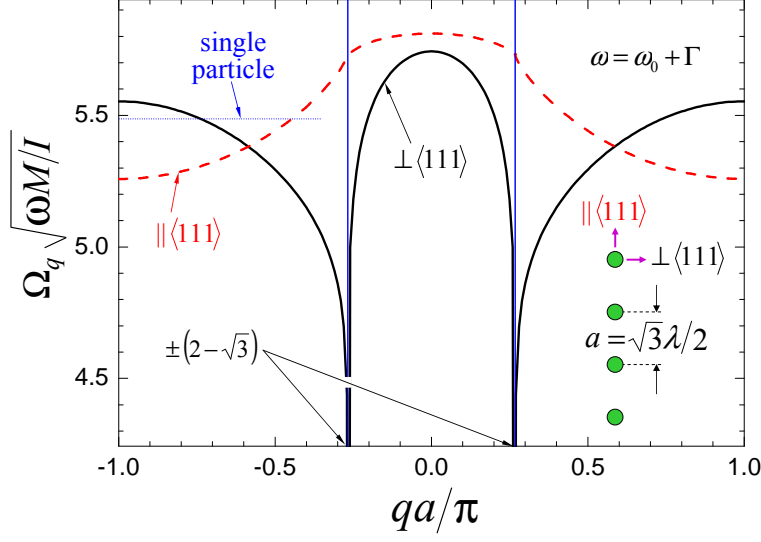


FIG. 2: Dispersion relation of the oscillation modes in an infinite periodic string of atoms located at the minima of electric field strength along the  $\langle 111 \rangle$  direction under the same conditions of illumination as in Fig. 1 (see lower inset in that Fig.; the coordinate axes are taken parallel to the laser beams). The nearest-neighbor distance is  $a = \sqrt{3}\lambda/2$ . The light frequency is tuned to  $\omega = \omega_0 + \Gamma$ , using the same notation and atomic polarizability as in Fig. 1. The oscillation frequency is given as a function of momentum  $q$  along the string within the one-dimensional first Brillouin zone. Oscillations parallel to the  $\langle 111 \rangle$  direction (broken curve) are decoupled from those along perpendicular directions (solid curve).

scattering matrix [30]. Analyses along these lines have been previously offered by the author for momentum transfer from a fast electron to a particle [31] and for neighboring effects in the interaction force between two arbitrarily-shaped particles [24]. Higher-order multipoles beyond the dipole yield a more complex expression for the force, but the quadratic dependence on the field exhibited by Eq. (1) is still maintained.

These conditions have been considered in Fig. 3 for a two-dimensional (2D) square array of silica beads (see upper inset) trapped in a field given by

$$\mathbf{E}^{\text{ext}}(\mathbf{r}, t) = 8 \Re \left\{ E_0 e^{-i\omega t} \right\} \left\{ [\sin(Qx) \hat{\mathbf{x}} + \sin(Qy) \hat{\mathbf{y}}] \sin(k_z z) \cos \theta + [\cos(Qx) + \cos(Qy)] \hat{\mathbf{z}} \cos(k_z z) \sin \theta \right\},$$

where  $\theta$  is the angle between the beam directions and the normal to the plane of the array,  $Q = k \sin \theta$ , and  $k_z = k \cos \theta$ . This system is experimentally challenging because it requires

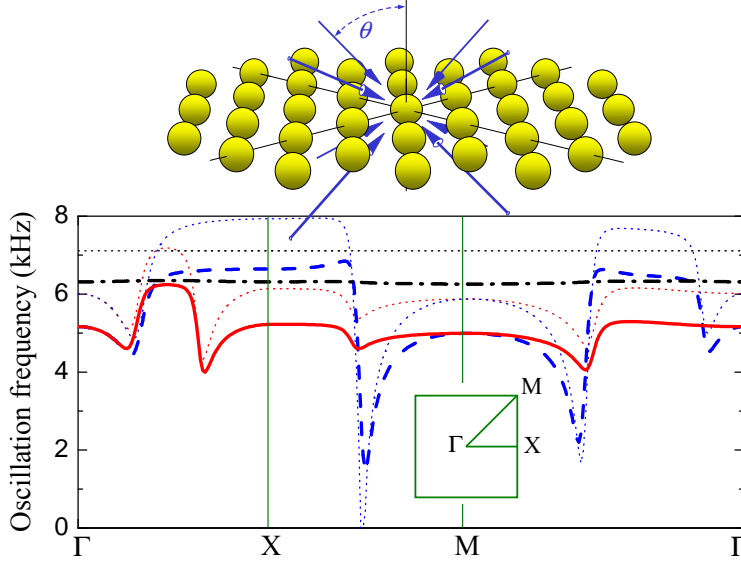


FIG. 3: Dispersion relation of oscillation modes in an optical lattice of silica spherical particles ( $\epsilon = 2.1$ ) in vacuum. The lattice is set up by four pairs of counter-propagating linearly-polarized beams with incident magnetic field in the plane of the particles. The inset shows the particles in their equilibrium positions forming a planar square lattice of nearest-neighbor distance  $\lambda/\sin\theta$ , where  $\theta = 50^\circ$  is the angle formed by the light beams and the normal to the plane of the array. Continuous, dashed, and dashed-dotted thick curves correspond to the three oscillation modes for each value of the parallel momentum along the excursion  $\Gamma X M \Gamma$  within the first Brillouin zone. The spheres diameter is 240 nm, the light wavelength is  $\lambda = 550$  nm, and the flux of each laser is  $100 \text{ W/cm}^2$ . These results are obtained with inclusion of higher-order multipoles beyond the dipole. Calculations in the dipole approximation (thin dotted curves) are shown for reference, with the polarizability obtained from the electric dipole Mie coefficient as  $\alpha = (3/2k^3) t_1^E$  [30].

to trap particles in vacuum, for which pioneering results were reported three decades ago by Ashkin and Dziedzic [32], who achieved optical levitation in high vacuum.

Three oscillation frequency bands are obtained and represented for an excursion along symmetry points within the first Brillouin zone of the reciprocal lattice in momentum space. One of the bands corresponds to nearly-independent-particle motion perpendicular to the plane of the array and is almost dispersionless (dashed-dotted thick curve). The remaining two bands (solid and dashed thick curves) are degenerate at the  $\Gamma$  and M points, which is a condition imposed by symmetry. Unlike the previous examples, the dielectric particles of Fig. 3 are attracted towards maxima of the light intensity (this is the equivalent of red-

detuned atomic resonances). The effect of multipolar interaction is quantitatively significant (cf. oscillation modes calculated in the dipole approximation, represented by thin dotted curves in Fig. 3; incidentally, these latter dipole calculations should describe well red-detuned atoms trapped in this optical-lattice geometry).

Low-frequency modes arising from long-range interactions are visible in Fig. 3 as pronounced dips that become very sensitive to finite array boundaries and size distribution of the particles. These effects have been phenomenologically described in Fig. 3 through a small attenuation in the interaction between distant particles represented by a dielectric function equal to  $1 + 0.03i$  in the surrounding medium, which gives an interaction decay-length of  $\sim 8$  times the nearest-neighbor distance.

## PHASE TRANSITIONS IN 1D OPTICAL MATTER

The above analysis has been limited to particles trapped at the sites of 3D lattices and capable of oscillating around their equilibrium positions. We shall now explore a different system comprised by particles that are confined along two spatial directions but free to move along the remaining third direction. This scenario is presented for instance in particles trapped inside a cylindrical optical cavity (e.g., a hole of a photonic crystal fiber), and also in particles confined to a 1D well of a 2D optical lattice like that of Fig. 4(a), in which the external field is

$$\mathbf{E}^{\text{ext}}(\mathbf{r}, t) = 4 \Re \left\{ E_0 e^{-i\omega t} \right\} [\cos(kz) + \cos(ky)] \hat{\mathbf{x}},$$

where  $E_0$  is the field amplitude of each laser. The particles will be assumed to have positive polarizability  $\alpha$  (i.e., the confinement occurs in regions of maximum electric field) and to be periodically spaced. This is a configuration of equilibrium for an infinite chain, in which the force acting on the particles vanishes. We shall then analyze the spectrum of collective oscillations within the first Brillouin zone of the reciprocal lattice and explore the stability of that equilibrium.

The self-consistent electric field amplitude acting on a given particle reduces from Eq. (3) to the analytical expression

$$E = \frac{4E_0}{1 - \alpha G_{q=0}^{\parallel}},$$

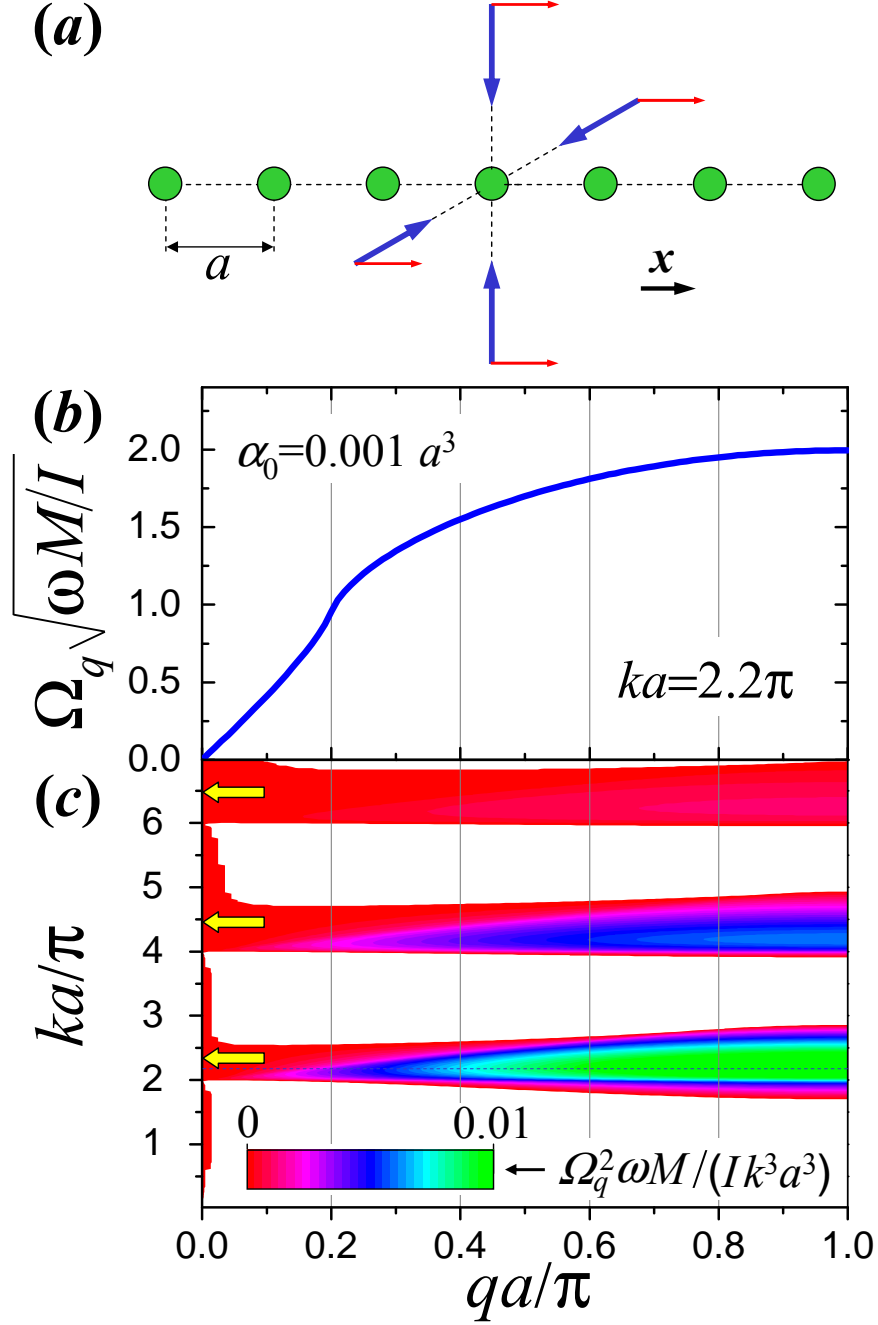


FIG. 4: Oscillation modes and stability of a linear array of particles trapped in a two-dimensional optical lattice set up by two pairs of counter-propagating beams with polarizations as shown in (a). The array is assumed to be periodic, infinitely long, and surrounded by vacuum. A typical spectrum of oscillations is presented in panel (b) for specific values of the free-space momentum of the trapping light  $k$  and the particle polarizability  $\alpha$ , normalized to the lattice spacing  $a$  (see text insets). The spectrum is given within the first Brillouin zone of momentum along the array  $q$ , with normalization of frequency and momentum as in Fig. 2. The contour plot of panel (c) represents squared oscillation frequencies as a function of  $q$  and  $k$  for  $\alpha = 1/(\alpha_0^{-1} - 2ik^3/3)$ , where  $\alpha_0 = 0.001a^3$  is the electrostatic polarizability (this prescription for  $\alpha$  is consistent with the optical

where  $G_{q=0}^{\parallel}$  [see Eq. (11)] is the sum of the fields scattered by the rest of the particles, and only the  $\exp(-i\omega t)$  component is considered. Small displacements out of equilibrium along small vectors  $\mathbf{u}_j$ , as defined at the beginning of Sec. , will then modify the self-consistent field in the vicinity of every particle  $j$  to

$$\mathbf{E}_j = \mathbf{E}^{\text{ext}} + \eta_j,$$

from which we discount the field scattered by that particle. The field perturbations can be conveniently obtained by expanding  $G(\mathbf{r})$  [see Eq. (4)] in Taylor series and by working in Fourier space  $q$  according to the definition

$$\eta_q = \sum_j e^{-iqaj} \eta_j,$$

similar to Eq. (10). We find

$$\eta_q^{\parallel} = \frac{g_q E}{\frac{1}{\alpha} - G_q^{\parallel}} u_q^{\parallel}$$

and

$$\eta_q^{\perp} = \frac{(-g_q E/2)}{\frac{1}{\alpha} - G_q^{\perp}} \mathbf{u}_q^{\perp},$$

where  $\parallel$  and  $\perp$  indicate directions parallel ( $\hat{\mathbf{x}}$ ) and perpendicular ( $\hat{\mathbf{y}}, \hat{\mathbf{z}}$ ) to the array, respectively,  $G_q^{\parallel}$  and  $G_q^{\perp}$  were defined in Eqs. (11) and (12), and

$$g_q = 4i \sum_{j=1}^{\infty} \sin(qaj) \frac{e^{ikaj}}{(aj)^4} [(kaj)^2 + 3ikaj - 3].$$

Finally, the oscillation frequencies  $\Omega_q$  are obtained from Newton's equation, similar to Eq. (9), but with a more complex expression for  $\Sigma_{\mathbf{q}}$ . Like in the system of Fig. 2, oscillations along parallel and perpendicular directions with respect to the array are decoupled and their frequencies reduce to

$$\Omega_q^{\parallel} = \left[ \frac{2|\alpha E|^2}{M} \Re \left\{ \frac{g_q^2}{1/\alpha - G_q^{\parallel}} + H_q^{\parallel} \right\} \right]^{1/2} \quad (13)$$

and

$$\Omega_q^{\perp} = \left[ \frac{2|\alpha E|^2}{M} \Re \left\{ \frac{g_q^2/4}{1/\alpha - G_q^{\perp}} + H_q^{\perp} \right\} + \frac{4k^2}{M} \Re \{ E_0^* \alpha E \} \right]^{1/2}, \quad (14)$$

respectively, where

$$H_q^{\parallel} = 4 \sum_{j=1}^{\infty} [\cos(qaj) - 1] \frac{e^{ikaj}}{(aj)^5} [i(kaj)^3 - 5(kaj)^2 - 12ikaj + 12]$$

and

$$H_q^{\perp} = 8 \sum_{j=1}^{\infty} [\cos(qaj) - 1] \frac{e^{ikaj}}{(aj)^5} [(kaj)^2 + 3ikaj - 3].$$

Perpendicular modes span a nearly-flat band around a high central frequency determined by the confining transversal potential [see the right-most term inside the square brackets of Eq. (14)]. The stability of the array will be exclusively determined by the band of longitudinal modes. A typical dispersion relation is shown in Fig. 4(b) for specific values of the polarizability (see inset) and spacing-to-wavelength ratio ( $a/\lambda = 1.1$ ). In contrast to the system of Fig. 2, the longitudinal band is acoustic, so that the oscillation frequency vanishes in the  $q \rightarrow 0$  limit (notice that  $g_q = H_q = 0$  in this limit), standing for a rigid slow translation of all particles along the 1D trapping well.

The stability of this type of array is analyzed in Fig. 4(c), which represents the oscillation spectrum given by Eq. (13) as a function of lattice spacing. White regions correspond to modes of imaginary frequency that describe motion beyond the validity of the harmonic approximation. The presence of these modes signals structural instabilities for some ranges of the period of the array, which must rearrange itself by creating defects with different particle separation. However, there are certain ranges of spacings that are stable, centered around the distance of equilibrium for a particle dimer in the channel (see horizontal arrows). This analysis of the array stability is also valid in the presence of friction forces, like those that would show up if the particles were immersed in a fluid. A practical realization of such arrays using holographic tweezers [13, 14] combined with transversal confining light would allow one to study their stability and to assess mechanical properties like the compressibility by fixing the position of the particles at the end of a finite array.

## CONCLUSION

Atoms and nanoparticles trapped in optical lattices have been shown to exhibit collective oscillations, the spectra of which reveal complex patterns that can be controlled by external illumination conditions. The oscillation frequency increases with the amplitude of the

binding lasers, thus adding an extra degree of freedom that allows obtaining frequencies in the kHz-MHz range in the case of atomic lattices. These oscillations constitute a genuine form of dynamical collective behavior in optical matter encompassing complex phenomena such as soft-modes and lattice phase transitions. Furthermore, our analysis of the oscillation spectra has been shown to resolve the question of the stability of the arrays.

The results presented here could be useful to design the following specific experiments:

- Collective motion in optical lattices of trapped atoms, which should be observable in their response to low-frequency radiation within the noted oscillation frequency range.
- Stability of 1D nanoparticle chains trapped along one channel of a 2D optical lattice. Initial particle trapping is possible using holographic illumination [14], superimposed to the optical lattice, and the stability could be proved by varying the relative intensity of holographic and optical-lattice laser beams.
- Phase transitions in optical matter, using a similar setup as in the previous point, but holding the ends of a chain at specific locations. Transitions should occur as these ends are displaced.

Finally, there are a number of open questions posed by these novel oscillations that will require separate developments, including the extension of this work to lower laser intensities and to conditions for which the oscillations behave as quasi-particles in atomic lattices. Interesting phenomena could also result from saturation effects at large laser intensities, whereby the atomic response is far from the linear regime. Equally important, thermodynamics of open systems like the arrays of Fig. 4 is expected to yield new properties associated to physical quantities such as the compressibility when exerting pressure on finite strings or the specific heat associated to the oscillations. These are challenges that will ultimately determine the applicability of collective behavior of optical matter to fields such as quantum information technology and signal processing.

## Acknowledgments

The author wants to thank M. Nieto-Vesperinas for enjoyable discussions. This work has been supported in part by the Spanish MEC (contracts FIS2004-06490-C03-02 and

NAN2004-08843-C05-05) and by the EU (STREP STRP-016881-SPANS and NoE Metamorphose).

- 
- [1] M. Greiner, O. Mandel, T. Esslinger, T. W. Hänsch, and I. Bloch, *Nature* **415**, 39 (2002).
  - [2] M. M. Burns, J.-M. Fournier, and J. A. Golovchenko, *Phys. Rev. Lett.* **63**, 1233 (1989).
  - [3] M. M. Burns, J.-M. Fournier, and J. A. Golovchenko, *Science* **249**, 749 (1990).
  - [4] P. Münstermann, T. Fischer, P. Maunz, P. W. H. Pinkse, and G. Rempe, *Phys. Rev. Lett.* **84**, 4068 (2000).
  - [5] B. Nagorny, T. Elsässer, and A. Hemmerich, *Phys. Rev. Lett.* **91**, 153003 (2003).
  - [6] D. Jaksch, J. I. Cirac, P. Zoller, S. L. Rolston, R. Côté, and M. D. Lukin, *Phys. Rev. Lett.* **85**, 2208 (2000).
  - [7] A. Ashkin, *Phys. Rev. Lett.* **24**, 156 (1970).
  - [8] C. A. Ashley and S. Doniach, *Phys. Rev. B* **11**, 1279 (1975).
  - [9] A. Ashkin, *Science* **210**, 1081 (1980).
  - [10] A. Ashkin and J. M. Dziedzic, *Science* **235**, 1517 (1987).
  - [11] P. M. Hansen, V. K. Bhatia, N. Harrit, and L. Oddershede, *Nano Lett.* **5**, 1937 (2005).
  - [12] M. Pelton, M. Liu, H. Y. Kim, G. Smith, P. Guyot-Sionnest, and N. F. Scherer, *Opt. Lett.* **31**, 2075 (2006).
  - [13] D. G. Grier, *Nature* **424**, 810 (2003).
  - [14] D. G. Grier and Y. Roichman, *Appl. Opt.* **45**, 880 (2006).
  - [15] M. Righini, A. S. Zelenina, C. Girard, and R. Quidant, *Nat. Phys.* **3**, 477 (2007).
  - [16] F. J. García de Abajo, T. Brixner, and W. Pfeiffer, *J. Phys. B* **40**, S249 (2007).
  - [17] N. K. Metzger, K. Dholakia, and E. M. Wright, *Phys. Rev. Lett.* **96**, 068102 (2006).
  - [18] S. A. Tatarkova, A. E. Carruthers, and K. Dholakia, *Phys. Rev. Lett.* **89**, 283901 (2002).
  - [19] M. Hoppenbrouwers and W. van de Water, *Phys. Rev. Lett.* **80**, 3871 (1998).
  - [20] J. P. Gordon and A. Ashkin, *Phys. Rev. A* **21**, 1606 (1980).
  - [21] R. Loudon, *The Quantum Theory of Light* (Oxford University Press, Oxford, 2000).
  - [22] P. Zemánek, V. Karásek, and A. Sasso, *Opt. Commun.* **240**, 401 (2004).
  - [23] M. Guillon, *Opt. Express* **14**, 3045 (2006).
  - [24] F. J. García de Abajo, *J. Quant. Spectrosc. Radiat. Transfer* **89**, 3 (2004).

- [25] T. M. Grzegorzczuk, B. A. Kemp, and J. A. Kong, Phys. Rev. Lett. **96**, 113903 (2006).
- [26] T. M. Grzegorzczuk, B. A. Kemp, and J. A. Kong, J. Opt. Soc. Am. A **23**, 2324 (2006).
- [27] F. Depasse and J. Vigoureux, J. Phys. D **27**, 914 (1994).
- [28] M. S. Safronova, C. J. Williams, and C. W. Clark, Phys. Rev. A **67**, 040303(R) (2003).
- [29] It should be noted that Rb has another resonance of width  $\Gamma = 2\pi \times 2$  MHz at 795 nm (frequency  $\omega_1$ ), which combined with the 780 nm resonance (frequency  $\omega_0$ ) gives an effective value of  $\Gamma = 2\pi \times 6$  MHz for light tuned far from this region ( $|\omega - \omega_0| \gg \omega_0 - \omega_1$ ). However, we are discussing here light tuned very close to the 780 nm resonance ( $|\omega - \omega_0| \ll \omega_0 - \omega_1$ ), for which the lower-frequency resonance can be overlooked.
- [30] F. J. García de Abajo, Phys. Rev. Lett. **82**, 2776 (1999).
- [31] F. J. García de Abajo, Phys. Rev. B **70**, 115422 (2004).
- [32] A. Ashkin and J. M. Dziedzic, Appl. Phys. Lett. **28**, 333 (1976).
- [33] B. T. Draine and P. J. Flatau, J. Opt. Soc. Am. A **11**, 1491 (1994).